Genetically-Encoded Neuronal Indicator and Effector (GENIE) Project

Steering committee (2016-2018)

Vivek Jayaraman, Group Leader

Douglas Kim, Program Scientist

Wyatt Korff, Associate Director and Program Scientist, Team Projects

Loren Looger, Group Leader

Eric Schreiter, Group Leader

Nelson Spruston, Scientific Program Director and Laboratory Head

Karel Svoboda, Group Leader

Research staff

Stephan Brenowitz, Senior Scientist (voltage sensor development)

Hod Dana, Research Specialist (mouse imaging)

Jeremy Hasseman, Research Specialist (molecular cloning)

Graham Holt, Research Technician (protein biochemistry)

Yi Sun, Research Specialist (*Drosophila* imaging)

Getahun Tsegaye, Research Specialist (molecular cloning)

Collaborating scientists

John Macklin, Senior Scientists, APIG, Janelia Research Campus

Misha Ahrens, Group Leader, Janelia Research Campus

Cornelia Bargmann, Rockefeller University

1.0 Summary

For more than 15 years, fluorescent proteins have been engineered to report neural activity. Neural circuits process information on spatial scales ranging from single synapses to large assemblies of neurons at time scales from milliseconds to months. Functional imaging based on fluorescent protein sensors spans all of these temporal and spatial scales. Protein sensors are now routinely used to image neuronal activity *in vivo* and they underlie many recent advances in cellular functional imaging. However, protein sensors still have major limitations as reporters of neural activity.

The GENIE project develops existing prototype protein sensors into the best-in-class tools for *in vivo* neurophysiology. Our focus is on high-impact sensors that will benefit from protein engineering and large-scale screening technology. The GENIE project will continue to optimize green and red calcium indicators. A major new program was recently initiated with the goal to engineer genetically-encoded voltage sensors.

2.0 Background

The goal of the GENIE Project is *to engineer fluorescent sensors for imaging of neuronal activity in the intact nervous system.*

2.1 Genetically-encoded calcium indicators (GECIs)

Understanding the function and plasticity of neural circuits requires measurements of neural activity over a large range of spatial and temporal scales. Calcium indicators have been especially useful for neurobiology. In most neurons, action potentials (APs) are tightly coupled to large (20-fold) and rapid (rise time <1 millisecond) increases in intracellular free calcium concentration. These calcium transients can be measured as fluorescence changes in neuronal somata (4, 12), dendrites (13, 14), and axons (15, 16) *in vitro* and *in vivo* as a proxy for the underlying electrical activity. Calcium indicators are also useful in non-spiking, graded potential neurons (17, 18), although the optimal indicator parameters may differ for different applications. Additionally, excitatory synaptic transmission is typically associated with large-amplitude (20- to 100-fold) increases in calcium concentration in small synaptic compartments (*e.g.* dendritic

spines). These synaptic calcium transients can be used to quantify synaptic transmission *in vitro* (19) and *in vivo* (9, 20). Calcium imaging therefore provides a versatile tool to probe neural activity over timescales of milliseconds to months and spatial scales of micrometers to millimeters.

GCaMP6 and beyond

GECIs occupy a niche complementary to single unit electrophysiology. GECIs can be used to monitor activity in large populations of neurons, but with limited dynamic range and temporal resolution. Single unit methods have better sensitivity, dynamic range and time resolution, but sample activity sparsely. A major goal of the GENIE Project is to optimize GECIs to achieve signal-to-noise ratios (SNRs) that rival electrophysiological methods. We have developed the general-purpose GFP-based GCaMP6 sensors (9), which under favorable conditions detect single spikes in neuronal populations *in vivo*. GECIs with even higher sensitivity will allow larger populations of neurons to be imaged more rapidly and under more challenging conditions (*e.g.* during behavior). High sensitivity comes at the price of limited dynamic range; high-sensitivity indicators saturate at modest activity levels, making them unsuitable for monitoring activity patterns in neurons with high spike rates. Existing GCaMP6 indicators are not sufficiently sensitive to measure single APs in some cell types, such as parvalbumin-positive interneurons in rodents. Beyond GCaMP6, we will develop a suite of green indicators tailored to specific applications, including detecting activity in large populations of neurons, single-spike detection across neuron types, measurement of spike rates over a wide dynamic range, and imaging spike times with high-speed indicators.

Red GECIs

Red fluorescent GECIs (21, 22) are of particular interest for four reasons. First, longer wavelength excitation light penetrates deeper into tissue and is absorbed much less than green fluorescence, especially in mammalian tissue. Red GECIs (R-GECIs) therefore promise deeper and less invasive *in vivo* imaging compared to green GECIs. Second, many transgenic animals expressing green fluorescent proteins have been created; R-GECIs can be used in these animals. Third, R-GECIs are more easily combined with channelrhodopsin-2 (ChR2)-based manipulations of neural circuits with the spectral separation necessary for simultaneous imaging and excitation.

Fourth, combinations of red and green GECIs promise simultaneous imaging of multiple distinct neural structures (23). We will thus continue developing a suite of sensitive R-GECIs by improving on existing scaffolds and leveraging the process we pioneered for green GECIs.

Long-term GECI expression

In mammalian systems, stable long-term expression of protein sensors remains a major challenge. High protein concentrations are required for *in vivo* imaging (GECIs, 10-100 micromolar) (24). Viral infection using AAV viral vectors is currently the gene delivery method of choice (7). Although AAV produces sufficient expression, expression levels continue to ramp up over months (6-fold from 1 to 6 months of expression) (9), eventually causing cytotoxicity and changes in neuronal behavior (7). GECIs can be expressed at constant levels over 10 months in transgenic mice, without signs of cytotoxicity (25, 26). We are developing transgenic mice for Cre-dependent gene expression, optimized for *in vivo* imaging (27). Equally importantly, we will optimize sensors for protein stability, which may provide several benefits: boosting expression levels, reducing cytomorbidity and decreasing levels of inactive sensor, which contributes to background fluorescence. In flies, fish and worms cytotoxicity is less often a problem, likely because the short lifecycle of these preparations does not require expression for longer than a few days.

2.2 Genetically-encoded voltage indicators (GEVIs)

We have initiated a program to engineer genetically-encoded voltage sensors. Calcium indicators are excellent tools for detecting neural activity, including action potentials. However they have limited dynamic range for quantifying spike rates. Calcium concentration changes are hard to interpret in terms of membrane potential dynamics in subcellular compartments such as dendrites. Voltage imaging promises to overcome these shortcomings. Voltage imaging keeps pace with high spike rates (28), is much faster than calcium imaging, and can measure subthreshold activity across the dendritic tree (29), including inhibitory input. Thus, tracking electrical activity using voltage sensors holds tremendous promise for imaging neurons and neural networks.

State of the art

Multiple types of fluorescent protein sensors of voltage have been developed. The earliest protein sensors consisted of fusions of voltage-gated channels and fluorescent proteins (30). More recently, the voltage-sensitive phosphatase domain (VSD) has been used in combination with one or more fluorescent proteins (31-33). In these sensors voltage-dependent movement of the membrane voltage sensor modulates fluorescence of a tethered fluorescent protein (FP) or FRET pair (34). ArcLight (33) and ASAP (35) belong to this class. Fluorescent protein-based probes are relatively bright but their response amplitudes are low ($\Delta F/F_0$ per spike ~ 20%). Several of these sensors become less fluorescent with depolarization (inverted response), which causes a serious SNR disadvantage when imaging densely labeled neurons with sparse activity patterns.

Another class of protein voltage sensors is based on microbial rhodopsin proton pumps, such as Archaerhodopsin-3 (Arch) (36). Retinal molecules in these rhodopsins serve as fluorophores. Voltage sensing is achieved through retinal isomerization, proton transfer, and accompanying fluorescence changes. Arch is a positive sensor and has high $\Delta F/F_0$ (~50%) and speed (rise $t_{1/2}$ ~ 1 ms). However, retinal quantum yield of fluorescence is ~ $1x10^{-5}$, and thus Arch requires 1000-fold higher illumination compared to GFP, which makes it difficult to use for imaging in thick specimens. Because the fluorescence properties of Arch are intrinsically linked to retinal it is unclear whether the fluorescence of Arch can be appreciably improved by protein engineering. In addition, some Arch variants retain proton-pumping activity that can perturb neuronal activity.

Some of the best features of opsin-based sensors and fluorescent protein-based sensors have been combined in electrochromic FRET (eFRET) voltage sensors, including QuasAr-FP and MacQ-FP (37, 38). These proteins couple a microbial rhodopsin with a tethered fluorescent protein. The design relies on spectral overlap of the fluorescent protein's emission and retinal's absorption. Current incarnations become dimmer upon membrane depolarization and show small signal changes.

Despite substantial effort, GEVI sensitivity for detecting activity at the level of single neurons is still vastly inferior to protein calcium sensors. This is in part due to fundamental constraints because voltage needs to be sensed across the lipid bilayer. Relatively few protein sensor molecules can be incorporated into the two-dimensional membrane (a typical density for

membrane proteins, 10 μm^{-2}, corresponds to 10^4 molecules in the somatic membrane). In contrast, calcium is sensed by 10^7 molecules throughout the somatic cytoplasm (50 μM) (24). Furthermore, voltage sensors change less than 2-fold for typical voltage changes, whereas GCaMP6 changes fluorescence up to 50-fold during physiological changes in intracellular calcium. Finally, FP-based sensors restricted to the membrane show limited diffusional recovery and therefore can suffer from photobleaching. Orders of magnitude improvements will be required to make voltage sensors competitive with GECIs for imaging of neuronal populations at cellular resolution, which is a core goal of the GENIE project.

3.0 Progress Report (September 2014-present)

In this section we only report on progress relevant to current work. For completed GENIE projects refer to GENIE publications (https://www.janelia.org/project-team/genie):

Dana *et al*., (2015) Sensitive red protein calcium indicators for imaging neural activity. *Submitted*.

Fosque BF, Sun Y, Dana H, Yang CT, Ohyama T, Tadross MR, Patel R, Zlatic M, Kim DS, Ahrens MB, Jayaraman V, Looger LL, & Schreiter ER. (2015) Labeling of active neural circuits in vivo with designed calcium integrators. *Science* 347:755-60.

Dana H, Chen TW, Hu A, Shields BC, Guo C, Looger LL, Kim DS, & Svoboda K. (2014) Thy1-GCaMP6 transgenic mice for neuronal population imaging in vivo. *PLoS One* 9:e108697.

Thestrup T, Litzlbauer J, Bartholomäus I, Mues M, Russo L, Dana H, Kovalchuk Y, Liang Y, Kalamakis G, Laukat Y, Becker S, Witte G, Geiger A, Allen T, Rome LC, Chen TW, Kim DS, Garaschuk O, Griesinger C, & Griesbeck O. (2014) Optimized ratiometric calcium sensors for functional in vivo imaging of neurons and T lymphocytes. *Nat Methods* 11:175-182.

Wardill TJ, Chen TW, Schreiter ER, Hasseman JP, Tsegaye G, Fosque BF, Behnam R, Shields BC, Ramirez M, Kimmel BE, Kerr RA, Jayaraman V, Looger LL, Svoboda K, & Kim DS. A neuron-based screening platform for optimizing genetically-encoded calcium indicators. (2013) *PLoS One* 8:e77728.

Chen TW, Wardill TJ, Sun Y, Pulver SR, Renninger SL, Baohan A, Schreiter ER, Kerr RA, Orger MB, Jayaraman V, Looger LL, Svoboda K, & Kim DS. (2013) Ultrasensitive fluorescent proteins for imaging neuronal activity. *Nature* 499(7458):295-300.

Akerboom J, Chen TW, Wardill TJ, Tian L, Marvin JS, Mutlu S, Calderón NC, Esposti F, Borghuis BG, Sun XR, Gordus A, Orger MB, Portugues R, Engert F, Macklin JJ, Filosa A, Aggarwal A, Kerr RA, Takagi R, Kracun S, Shigetomi E, Khakh BS, Baier H, Lagnado L, Wang

SS, Bargmann CI, Kimmel BE, Jayaraman V, Svoboda K, Kim DS, Schreiter ER, & Looger LL. (2012) Optimization of a GCaMP calcium indicator for neural activity imaging. *J Neurosci* 32:13819-13840.

3.1 GECI assays

Screening in cultured neurons

Underlying the development of GCaMP6, red GECIs and other advances in GECI development has been a neuronal culture assay for characterizing GECI variants rapidly in the relevant cell type (**Fig. 1A-C**). This was necessary because neurons have fast and small-amplitude calcium accumulations that are difficult to model in non-neuronal systems. Primary neuronal cultures in 96-well plates are transfected with GECI variants and a nuclear fluorescent protein to control for expression level. Action potentials (APs) are triggered using extracellular stimulation electrodes, while neurons are imaged using widefield fluorescence microscopy. The output of the assay is the fluorescence dynamics of multiple individual neurons to a variety of trains of APs (39). This assay therefore allows characterization of large numbers of GECI variants under relevant conditions.

We have quadrupled the throughput of our assay (December 2010: 0.99 variants tested/day; October 2015: 4.5 variants tested/day). A major change is that gene transduction is now accomplished by DNA electroporation into primary neurons instead of viral infection. Transfections are performed using a liquid handling robot. Screening is now performed in 96-well format instead of 24-well format.

We mutagenize scaffolds using gene assembly cloning methods (40). Amino acid positions are selected for mutagenesis based on the crystal structures of sensors (10, 11, 41). Substitutions are made at single positions using 19 separate mutagenic primers costing ~$30 per substitution (without labor) including sequence verification. Mutants are then tested in the culture assay, and the best point mutants are combined. Individual clones are assayed in multiple wells.

The sensitivity of the neuronal culture assay is limited by v ariability in neuronal physiology. A 100% improvement over R-GECO1.0 or GCaMP3 can be detected for a 1AP response with eight replicates ($p<0.01$). The assay cost is $6 per variant (without labor). Throughput is limited by the

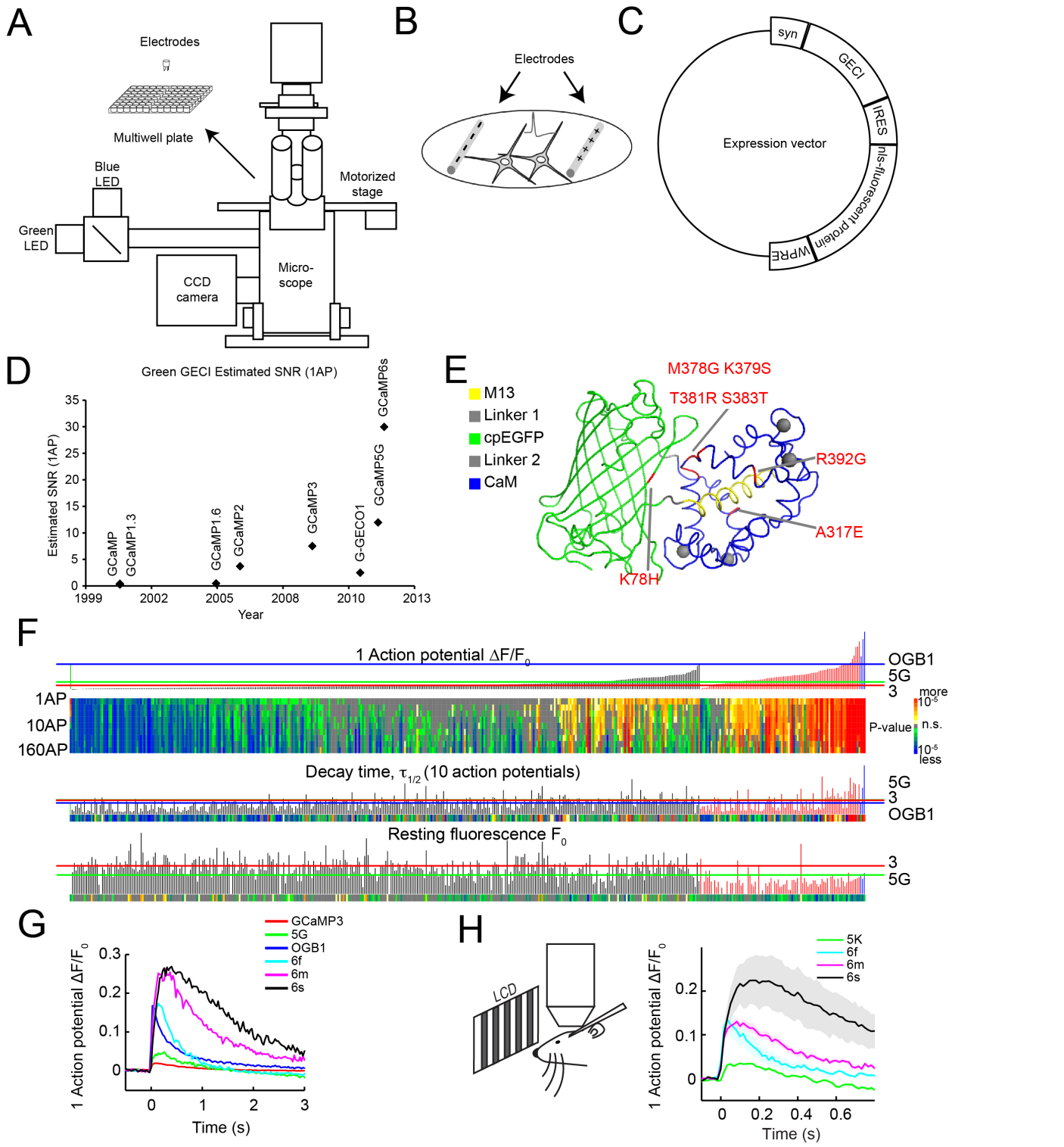

Figure 1. GCaMP6 engineering.
(A) Neuronal culture screening platform. (B) Schematic of stimulation geometry. (C) Expression vector with human *synapsin-1* promoter (syn), GECI variant, internal ribosome entry site (IRES), nuclear localization signal fused with fluorescent protein (nls-fluorescent protein), and woodchuck hepatitis virus post-transcriptional regulatory element (WPRE). (D) Optimization of GCaMP for detecting neuronal activity. GCaMP SNR after 1AP was estimated for GCaMP, GCaMP1.3, GCaMP1.6, GCaMP2, GCaMP3, G-GECO1, GCaMP5G, and GCaMP6s. Note that SNR was estimated across different types of assays published by multiple groups and is thus a rough estimate. Data from (1-9). (E) GCaMP structure (10, 11) and mutations (red) found in different GCaMP6 variants. CaM-binding peptide M13 from myosin light chain kinase (M13, yellow), linker 1 (gray), circularly-permuted EGFP (cpEGFP, green), linker 2 (gray), CaM (blue), calcium ions (gray spheres). (F) Screening results for GCaMP6. Top, fluorescence change in response to 1 AP (vertical bars, $\Delta F/F_0$; green bar, OGB1-AM, left; black bars, single GCaMP mutations; red bars, combinatorial mutations; blue, GCaMP6 indicators) and significance values for different AP stimuli (color plot). Middle, half decay time after 10 APs. Bottom, resting fluorescence, F_0 normalized to nuclear mCherry fluorescence. Red line, GCaMP3 level; green line, GCaMP5G level; blue line, OGB1-AM level. (G) Single AP Responses averaged across multiple neurons and wells for GCaMP3, 5G, 6f, 6m, 6s, and OGB1. (H) GCaMP6 performance in the mouse visual cortex in response to a single spike. Left, schematic of the experiment. Right, median fluorescence change in response to 1 AP for different calcium indicators. Shading corresponds to s.e.m., n = 9 (GCaMP5K, data from (8)), 11 (GCaMP6f), 10 (GCaMP6m), 9 (GCaMP6s) cells. GCaMP5K and GCaMP5G have similar properties.

cloning rate (7.7 constructs cloned/day for RCaMP and R-GECO; an improvement of a factor of 6 over the GCaMP cloning rate, 1.3 constructs cloned/day). Currently the neuronal culture assay has excess capacity that could be used for suitable collaborations or additional projects.

Assaying GECIs in vivo

GECIs are routinely tested in the mouse visual cortex in response to drifting grating stimulation (9, 25, 26, 42, 43) (**Fig. 1H**). We have validated the performance of GECIs in adult *Drosophila* by comparing odor responses in projection neurons (PNs) of the fly antennal lobe (9), and in the larval *Drosophila* NMJ (Fig. 3). In addition we have also developed a visual system assay, using fly lamina and lobula plate neurons **(Fig. 2**). Lamina neurons respond to changes in luminance with fast transients, providing a useful benchmark for the performance of kinetic variants of GECIs in non-spiking fly neurons. We have also identified a spiking optic lobe interneuron that exhibits a wide range of spike rates in response to visual stimulation. The neuron's large size permits simultaneous electrophysiology and calcium imaging experiments, which we use to quantify GECI performance *in vivo*.

3.2 Sensitive and fast GCaMPs

We developed the general-purpose GCaMP6 family of indicators with improved SNR for spike detection *in vivo* **(Fig. 1D-H**) (9). GCaMP6 is based on close to 500 structure-guided mutations, with as many as 11 combined mutations in GCaMP3. GCaMP6s and GCaMP6f are the *de facto* standard GECIs in the field. In 2013, the GCaMP6 indicators were amongst the most widely requested reagents at Addgene.org (792 GCaMP6s requests as of October 2015) and the University of Pennsylvania Viral Vector Core. GCaMP6-expressing flies were amongst the most requested fly strains at the Bloomington *Drosophila* Stock Center (211 20XUAS-GCaMP6m requests as of October 2015; most requested stock out of 37,125 stocks in 2013).

Beyond GCaMP6, we have begun to engineer GCaMP6 variants with low resting fluorescence, to maximize SNR for large-scale *in vivo* imaging in rodents, higher resting fluorescence for applications in flies, and GCaMP6 variants with varying calcium affinities and binding cooperativity, to enable activity imaging in neurons with graded responses and fast-spiking neurons (**Fig. 3**). In the fly larval neuromuscular junction (NMJ) assay, GCaMP6 responses were

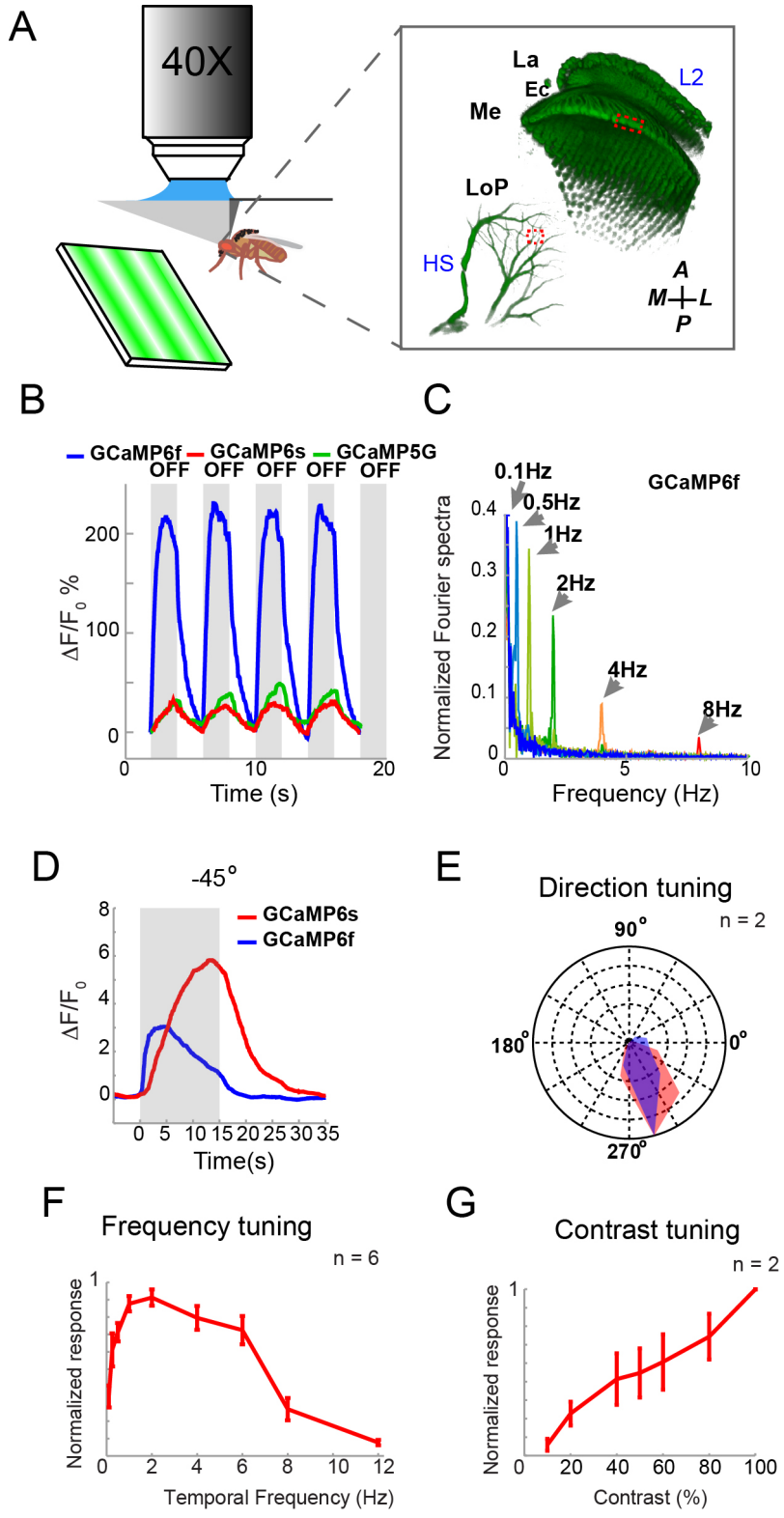

Figure 2. Fly visual system assay.
(A) Schematic of the fly visual assay. Female flies (3-5 days old) are glued onto a custom-built pyramid and 2-photon imaged through a window in the cuticle on the head. Visual stimulation is delivered through a modified digital-mirror-device that reflects a dispersed laser beam (532nm, DPSS) onto a pattern on a screen in front of the fly. A signal is also acquired from a silicon photodiode that detects changes in light intensity to synchronize visual stimulation with imaging. Laser light is isolated from GCaMP fluorescence through spectral filtering and physical masking. Inset: Schematic of the optic lobe, including lamina (La) monopolar cell L2, where the axons terminating in the second layer in the medulla (Me) are imaged (dashed rectangle); and the lobula plate (LoP) tangential cell HS, where dendritic trees are imaged (dashed rectangle). (B) GCaMP6f is faster and more sensitive than GCaMP6s and GCaMP5G in L2. L2 is a graded potential neuron that depolarizes in response to light offset. Whole-field flickering with different durations and duty cycles are used as visual stimulation. Gray bars denote light offset. (C) GCaMP6f responses to whole-field flickering visual stimulation flashed at various frequencies. (D) Representative traces of GCaMP6s and GCaMP6f in the HS neuron to moving gratings tilted at different angles, moving at different speeds and with different contrast (single condition shown). In these large non-spiking neurons, GCaMP6s responses are larger than GCaMP6f. GCaMP6f captures the stimulus onset and offset and is more similar to the envelope of the intracellular recording curves of this neuron. (E) Direction tuning of the imaged dendritic area of HS neuron measured with GCaMP6f (blue) and GCaMP6s (red). (F) Frequency tuning of the imaged dendritic area of HS neuron measured with GCaMP6s. (G) Contrast tuning of the imaged dendritic area of HS neuron measured with GCaMP6s.

as much as 3-fold increased over those of GCaMP5G with single AP stimulation, but responses were not improved at higher frequencies (80-160 Hz, **Fig. 3C**). For calcium imaging over a wider range of stimuli in fly neurons, we are engineering: (1) a series of 5-10 lower affinity indicators with different K_d's from 500 nanomolar to 10 micromolar that extend across the calcium range of various types of fly neurons, and (2) a single indicator with a GCaMP6s-like calcium K_d, but a Hill slope of 1 to 1.5, while maintaining GCaMP6s SNR levels. So far, we have tested 26 mutations at one or more of 4 calcium-binding sites of CaM and the M13/CaM interface that have been previously demonstrated to lower affinity and cooperativity (44). The most promising variants were tested in the fly NMJ assay, and found that they show linear increases in fluorescence at high firing rates that evoked saturating fluorescence responses in GCaMP6s (**Fig. 3C**). This series of indicators may allow instantaneous spike rates to be tracked in neurons with high spike rates.

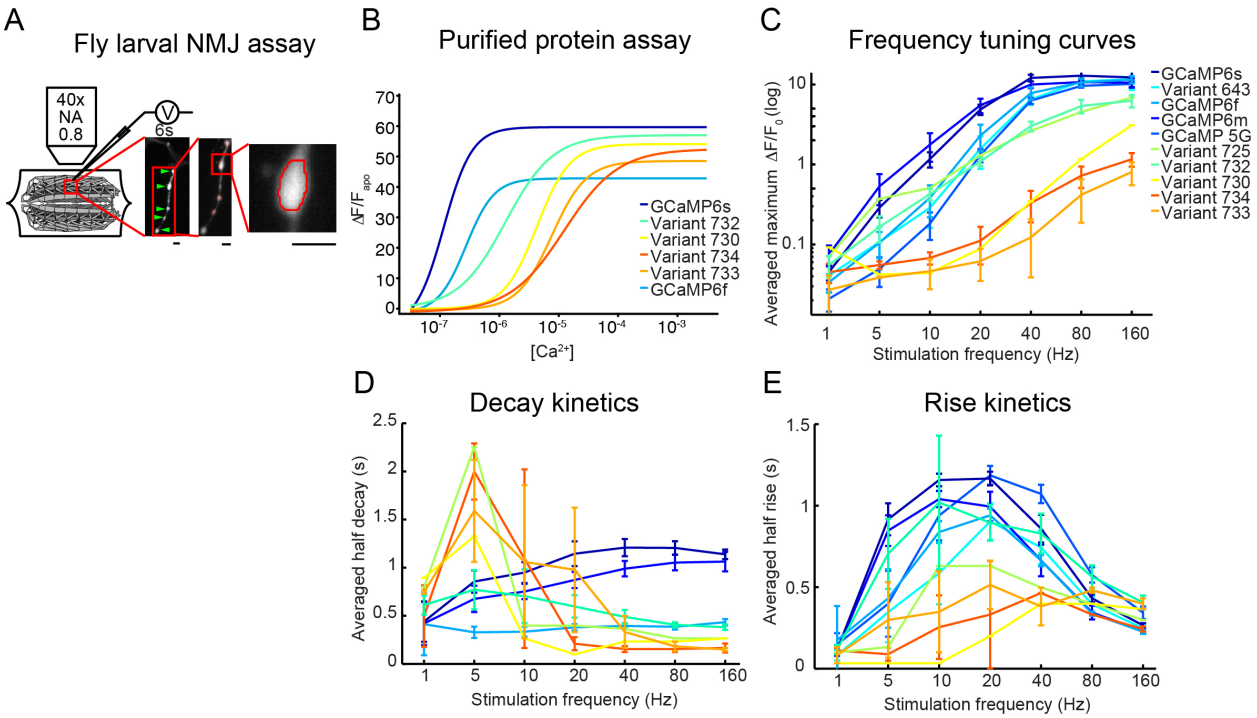

Figure 3. GCaMPs with varying affinity and cooperativity.
(A) Schematic and representative traces of the NMJ assay in *Drosophila* larvae. In a fillet preparation, motor neuron axons are cut and electrically stimulated with a suction electrode, and type Ib/s boutons are wide-field imaged with an EMCCD camera. Images are segmented and analyzed in response to stimulation. Scale bars, 5 µm. (B) Fluorescence changes ($\Delta F/F_{apo}$) from calcium titrations of purified GCaMP protein variants. (C) Frequency tuning curves for low affinity variants (EF-hand mutants), GCaMP6, and GCaMP5G. The averaged maximum $\Delta F/F_0$ at different stimulation frequencies are plotted. Different variants are color-coded according to their rank order of dissociation constant (K_d). Note that the low affinity variants are right-shifted and have shallower slopes. (D) Decay kinetics for the low affinity variants, GCaMP6, and GCaMP5G. The low affinity variants are faster than previous GCaMPs including GCaMP6f. (E) Rise kinetics for the low affinity variants, GCaMP6, and GCaMP5G. The low affinity variants are faster than previous GCaMPs including GCaMP6f.

3.3 Red GECIs

We have focused on optimizing two scaffolds, RCaMP and R-GECO, which are based on mRuby (45) and mApple (46), respectively. R-GECO1.0 is more sensitive than RCaMP1h (21). However, mApple-based GECIs exhibit photoswitching (46) when illuminated with blue light, leading to a transient increase of emitted red fluorescence. This artifact can limit the use of mApple-based GECIs together with optogenetic tools (21, 47). This is the principal reason for developing both scaffolds in parallel. We performed large-scale structure-guided mutagenesis and neuron-based screening (39) to develop improved red GECIs, starting with the RCaMP1h (21) and R-GECO1.0 (22) scaffolds.

Overall, the strategy employed is similar to GCaMP6 (9). Libraries of point mutations were generated in a structure-guided manner (21). Targets for mutagenesis included the calcium-binding domains, the binding pocket in CaM for M13, and the interface between CaM and fluorescent protein. In total, 934 RCaMP and 692 R-GECO single mutations were characterized in a neuronal culture assay thus far. Beneficial mutations were combined in a second round of mutagenesis (136 RCaMP1h and 163 R-GECO1). Based on the screen two new mRuby-based sensors, jRCaMP1a and jRCaMP1b, and one mApple-based sensor, jRGECO1a, were selected for release (cDNAs available at Addgene.org on 4/9/2015; AAV available at Penn Viral Vector Core on 9/15/2015; flies available at Bloomington Drosophila Stock Center on 9/15/2015) and further biophysical analysis and testing in intact systems. Red GECIs have been tested extensively in the mouse visual cortex, the fly NMJ, trigeminal sensory neurons in zebrafish (in collaboration with the Ahrens lab, Janelia Research Campus), and in ASH neurons of *Caenorhabditis elegans* (in collaboration with the Bargmann lab, Rockefeller University). jRGECO1a shows 6-fold improved sensitivity (1 AP detection) compared to its parent construct. jRCaMP1a is improved by 20-fold. Please see Dana *et al*., 2015 (submitted) for additional information including data.

Our testing implies that our R-GECIs are best-in class and will be useful for brain research. However, compared to GFP, red fluorescent proteins, and the derived red calcium sensors, still suffer from lack of photostability and brightness. Moreover, in experiments requiring long-term expression an immature (or dead-end side-reaction) green protein isoform accumulates that

degrades performance. We believe that R-GECIs based on other red fluorescent proteins may be the fastest way to make progress. It is likely that some form of chromophore environment "grafting" followed by extensive optimization may suffice, rather than starting anew from each scaffold.

3.4 Transgenic/Targeted Mice

GCaMP6s and GCaMP6f transgenic mice were produced using *Thy1*-GCaMP6-WPRE (48) and *Camk2a*-GCaMP6 (49) expression cassettes. Most founders (>25 lines) showed negligible expression. Five *Thy1* mouse lines were found suitable for *in vivo* imaging, with high expression levels in the hippocampus, neocortex, and other structures. Neurons did not show any cytopathology even after long-term expression of GCaMP6. These mice have been made available at The Jackson Laboratory. Unfortunately, *Thy1* mice show inconsistent expression patterns across brain regions and neurons. Thus each line is suitable only for a subset of brain areas. A stable, retargetable, and tunable (*i.e.* allowing expression levels higher than *ROSA26* mice) strategy for mouse transgenesis is needed for *in vivo* imaging.

3.5 GEVIs

We have developed a high-throughput screening method for improving GEVIs (see further below). We have tested ~ 4,000 variants of the ArcLight-Q239 GEVI and discovered several improved sensors with higher amplitude and faster responses.

4.0 Research Plan

4.1 Specific Aims for the Next Project Period

4.1.1 GCaMPs

(FY2016 commitment: 25%, FY2017 commitment: 25%, FY2018 commitment: 10%)

- Engineer and characterize 500 additional GCaMP variants.
- Screen for high SNR GCaMP variants.
- Screen for GCaMP variants with lower affinity and Hill coefficient.
- Screen for fast GCaMP variants.
- Develop and test low-F_0 variants for imaging large tissue volumes.

- Develop and test higher-F_0 variants for imaging in the fly brain.
- Develop a protein stability assay and screen for stable GCaMP variants.
- Test the 10 best variants *in vivo*.

4.1.2 R-GECIs

(FY2016 commitment: 33%, FY2017 commitment: 33%, FY2018 commitment: 33%)

- Engineer and screen 1,000 RFP-based calcium indicator variants.
- Screen for sensitive, fast, photostable and improved-maturation variants.
- Develop and test higher-F_0 variants for imaging in the fly brain.
- Test multi-population imaging by combining R- and G-GECIs in adult fly.
- Test the 10 best variants *in vivo*.

4.1.3 Transgenic/Targeted Mice

(FY2016 commitment: 9%, FY2017 commitment: 9%, FY2018 commitment: 7%)

- Engineer mice with high and stable neuronal expression of jR-GECO1a.

4.1.4 GEVIs

(FY2016 commitment: 33%, FY2017 commitment: 33%, FY2018 commitment: 50%)

- Benchmark existing scaffolds.
- Establish a high-throughput platform for evaluating protein voltage sensors.
- Engineer and screen 100,000 voltage sensors.
- Test most promising 200 variants in cultured neurons.
- Validate most promising hits with patch-clamp.
- Test 10 best variants in mouse, *Drosophila*, and zebrafish *in vivo*.

4.2 Experimental Plan

4.2.1 GCaMPs

Sensitive GCaMPs

The SNR of GECIs is largely determined by the fluorescence change per unit of activity (*i.e.* an AP, or a synaptic input) (50-52). This fluorescence change, $\Delta F/F$, in turn depends on the brightness of the calcium-bound bright form, the fraction of indicator that is calcium-bound, and

the brightness of the calcium-free indicator. Increasing ΔF/F can be achieved by tweaking three parameters:

1) Increase the affinity for calcium. This causes a larger ΔF/F per AP if spike rates are low. Increasing affinity was a major part of the GCaMP6 design strategy (9). One drawback of further pushing in this direction is that small stimuli will bring the indicator close to saturation, reducing the effective dynamic range.

2) Maximize fluorescence of the calcium-bound indicator. Screening for higher QE was also part of the GCaMP5 (8) and GCaMP6 (9) design strategies. However, the brightness of calcium-bound GCaMP6 is already higher than GFP and it is therefore unlikely that this parameter will yield additional improvements.

3) Minimize resting fluorescence. Our screen has revealed linker mutations with reduced resting fluorescence, without a large reduction of the peak fluorescence. In the past we have not focused on these mutations because our strategy was to produce indicators with appreciable resting fluorescence, which is critical for structural imaging. However, transgenic animals now allow imaging in a background in which neurons, nuclei, or other structures of interest are labeled with red fluorescence protein, obviating the need for substantial resting fluorescence (53). Reducing resting fluorescence even by a factor of two will have a substantial impact on SNR, increasing the yield in cellular imaging experiments by several-fold. We believe that this is the most fruitful path forward. We will therefore create GCaMPs with low resting fluorescence for large-scale, high SNR imaging. 200 linker variants of GCaMP6s and 6f will be screened. We aim to engineer variants maintaining the peak fluorescence of GCaMP6s and 6f, while lowering F_0 by 5-fold.

In flies, where it is common to use GAL4 drivers to target GECIs to sparse neural populations in neuropil (rather than cell bodies), substantial resting fluorescence remains desirable to easily locate and identify neural structures for imaging. Higher resting fluorescence is particularly important in behaving flies, in which high illumination intensity can artificially excite neural tissue and result in behavioral artifacts. In addition, the use of a co-labeling FP (*e.g.* RFP) complicates the use of multiple GECIs for simultaneous imaging of disparate neural populations. Thus, moderate-to-high resting fluorescence will continue to be a consideration when screening GCaMPs and R-GECIs for use in *Drosophila*.

Stable GCaMPs

GCaMP6 sensors have to be used at high concentrations (approximately 10-150 micromolar) for *in vivo* imaging (24). These protein concentrations are among the highest normally achieved in the brain and are difficult to mimic in transgenic mice. Instead GCaMPs are typically delivered using viral vectors such as AAV. AAV-mediated expression has undesired consequences. Protein expression increases monotonically with time, ultimately leading to cytotoxic GCaMP concentrations. The high expression levels required interfere with expression and/or function of endogenous proteins. Protein concentrations depend on the rate of production and the rate of degradation. To increase protein concentrations without increasing expression, we will engineer GCaMPs with increased protein stability. We anticipate that more stable GCaMPs will allow higher protein concentrations at modest expression rates, increasing the fraction of total protein that is fully-functional, rather than misfolded (yet fluorescent). This will allow use of transgenic methods for expression and imaging with reduced cytotoxicity.

We will test 200 more GCaMP6s and 6f variants to improve protein stability. This will include altering potential ubiquitination sites, improving thermodynamic stability, and optimizing codon usage for mice and flies. In addition, GCaMP6 will be circularly permuted to place the split GFP halves at the N- and C-termini to improve translation efficiency. Variants will be screened by transient transfection of HEK293T cells, application of a protein synthesis inhibitor (cycloheximide), and then epifluorescence imaging or fluorescence-activated cell sorting (FACS) to measure GCaMP variant fluorescence and fluorescence of a co-expressed mCherry control. We will also directly measure extent of degradation through the proteasomal pathway, through use of inhibitors such as lactacystin (7). The goal will be to achieve a 5-fold increase in stability leading to a 5-fold increase in protein concentration, while maintaining GCaMP6 SNR levels. The best variants will be tested in cultured neurons and *in vivo* in mice and flies.

Linear GCaMPs

Although it may not be possible to reduce the Hill coefficient to the level of the best synthetic indicators (*e.g.*, OGB1, with Hill coefficient of 1) and produce linear responses across low and high calcium concentrations, we hope to produce a family of indicators with different K_d's that span the dynamic range of typical neuronal firing rate regimes and calcium concentrations. Initial

testing in the fly NMJ suggests that the kinetics of lower K_d mutants may allow instantaneous firing rates to be tracked in high-firing-rate neurons. We will codon-optimize the best mutants for the fly to increase basal fluorescence, and then test these variants *in vivo* in the adult fly visual system.

Milestones

For FY2016, we will engineer low-F_0 GCaMPs such that 5-fold more neurons can be imaged *in vivo* with GCaMP6s-like SNR for mouse and limited fly applications. Stable GCaMPs will be produced that have 5 times greater stability of GCaMP6 when expressed *in vivo* and are less toxic. GCaMPs with lower calcium affinity and cooperativity will be made that span the calcium ranges of various fly high frequency and non-spiking neurons for improved activity detection. For FY2017, the best low affinity, high- F_0 variants will be tested *in vivo* in fast-spiking neurons of the adult fly visual system.

4.2.2 R-GECIs

We propose to engineer improved red calcium sensors beyond jRCaMP1a,b and jRGECO1a. After making considerable gains in amplitude and speed (Dana *et al*., 2015 submitted), we will next address the following design parameters:

Peak brightness is an easily measurable parameter that is highly relevant to imaging. It is proportional to the QE and related inversely to the bleaching cross-section (54). We will maintain $\Delta F/F_0$ and increase peak brightness. So far our protein engineering has focused on sites away from the chromophore of RCaMP and R-GECO. We will first identify highest SNR and highest SNR/highest speed variants and then mutate near the chromophore. We believe that given the high level of sequence homology between red FPs it should be possible to graft chromophore-forming residues and surrounding side-chains from recently improved FPs (*e.g.* mCrimson, mCardinal) without having to start from scratch with the new scaffolds. It is likely that subsequent optimization will be required after chromophore grafting, but such designs may improve brightness or photostability in an efficient manner. Photophysical measurements will be performed in collaboration with the JRC Applied Physics and Instrumentation Group (APIG) in *E. coli* lysate or partially-purified protein preparations (John Macklin). The goal will be obtain

improvements in photobleaching rates and photoswitching. Spectral separation from green fluorescent calcium indicators will also be tested. We will also explore long Stokes shift R-GECIs that can be co-excited with GCaMP but yield easily separable emission.

Lower F_0 for improved imaging of neuronal populations. We seek to lower the background fluorescence from inactive neurons and processes in order to increase SNR. A co-expressed GFP could be used to identify sensor-expressing neurons *in vivo*. Re-engineering of the M13/FP and FP/CaM linkers will be done to lower F_0 while maintaining the peak fluorescence, similar to the strategy for low-F_0 GCaMPs. The goal will be to increase SNR so that thousands of neurons *in vivo* can be imaged simultaneously at high speed in mouse brains.

Spectral purity. Improving the spectral purity of red fluorophores is related to photoswitching and lowering F_0 discussed above. Contaminating fluorescent species that absorb at 900 nm and emit in the green and red bands are present in the RCaMP1h- and R-GECO1.0-derived sensors. These become apparent after long-term expression by AAV infection in mice (Dana *et al*., 2015 submitted). These protein species are not modulated by calcium, but they contribute non-productively to the F_0 and thus reduce the overall $\Delta F/F_0$. Chromophore engineering by point mutation or grafting will also be employed to address this issue. It may be necessary to adopt a different red protein with better long-term behavior *in vivo*. Spectral purity is critical for applications involving the simultaneous use of red and green GECIs in overlapping neural processes. This is particularly relevant for the fly, where most imaging is performed in neuropil rather than somata.

Lower affinity for wider dynamic range in fly neurons. The gains in RCaMP and R-GECO response amplitudes have been obtained through driving the apparent calcium K_d to lower levels than for the parent sensors. The response amplitudes are improved for low numbers of action potentials. But for high numbers of APs, responses are not much improved. By mutating individual or several of the 4 calcium-binding domains in CaM, we will create an affinity series of RCaMP and R-GECO sensors. Our goal is also to widen the dynamic range of calcium detection by reducing the cooperativity of calcium binding, together with improvements in maximal $\Delta F/F$.

Milestones

For FY2016, jRCaMP1 and jRGECO1 variants will be produced with these properties: lower F_0 to reduce background signal for improved population imaging, and lower affinity for activity monitoring of high frequency fly neurons. For FY2017, red calcium sensors with improved photostability and spectral purity will be developed. For FY2018, the best low affinity and improved chromophore variants will be tested in flies and mice.

4.2.3. Transgenic/targeted mice

We will optimize the *Rosa26*-CAG-lox-STOP-lox-GCaMP6s-WPRE expression cassette to increase expression levels. Linker sequences between the CAG promoter and sensor start codon will be re-engineered to allow for more efficient transcription and/or translation. Thousands of constructs with altered linker sequences will be tested for expression level in transient transfection assays in HEK293T tissue culture cells by epifluorescence imaging and FACS. A Cre recombinase-expressing construct and co-expressed RFP control (to normalize for transfection level) will be transfected transiently. The *Rosa26*-CAG variants with the highest fluorescence will be selected for use in gene targeting and mouse production for next generation GCaMPs, RCaMPs, and R-GECOs. In the absence of an improved strategy, we will continue using *Thy1* transgenic expression cassettes and selecting for founder lines with suitable expression patterns and levels. We will also continue using improved expression systems (*e.g.* TIGRE insulator, Tet-regulatable, lox-gated system (55)) in collaboration with other laboratories.

Milestones

For FY2016, engineer mice with high and stable neuronal expression of jR-GECO1a. In addition, thousands of *Rosa26*-CAG-lox-STOP-lox-GCaMP6s-WPRE variants will be screened in tissue culture cells. For FY2017, *Rosa26*-targeted mice with optimized cassettes will be produced with high and stable GCaMP6s, GCaMP6f, RCaMP, and R-GECO expression levels comparable to AAV-mediated expression in cortical neurons. For FY2018, expression analysis of targeted mice will be conducted.

4.2.4 GEVIs

To date, GEVI testing has been done only with modest numbers of variants (dozens). We are performing a large-scale mutagenesis screen to develop better GEVIs (**Fig. 4, 5**). Based on

available information it is not possible to predict which existing scaffold holds the greatest promise for improvements with large-scale engineering and screening. Over the next year we therefore plan to divide our resources across several scaffolds, roughly as follows: 40% ASAP1, 40% ArcLight, 20% other scaffolds, including new scaffolds as they become available. The first phase of screening has focused on ArcLight variants.

Our goals are to improve voltage sensors for various imaging applications *in vivo*. Parameters for improvement include:

Sensitivity - maximizing fluorescence change per voltage step is the primary parameter to be optimized in screening; positive fluorescence change is preferred.

Speed – fast sensors can track high spike rates; slower sensors are preferred to report subthreshold membrane potential dynamics; fast and slow sensors will be developed.

Localization - maximizing sensor localization to the plasma membrane while minimizing non-productive intracellular fluorescence (*e.g.* endoplasmic reticulum and endosome accumulations) to improve effective signal-to-noise ratio.

Brightness/photostability – these parameters relate to sensitivity; in addition, diffusion of sensors in the membrane is relatively limited, and thus engineering photostable molecules is a key goal.

Linearity – a linear relationship between fluorescence and voltage allows for more accurate membrane potential quantitation; on the other hand, a supra-linear relationship (such as occurs with GCaMP6) could provide more sensitive detection of spikes.

Toxicity/activity perturbation - a priority will be to engineer out phototoxicity as well as cytotoxicity.

Voltage sensor mutagenesis

Engineering variants to be screened for improved properties is achieved by mutating voltage sensor proteins. Mutagenesis is conducted in both a site-directed and unbiased manner using mismatched oligonucleotides and error-prone PCR, respectively. Voltage sensor variants are transfected in 96-well plates (**Fig. 5**). Our standard DNA vector includes a strong promoter

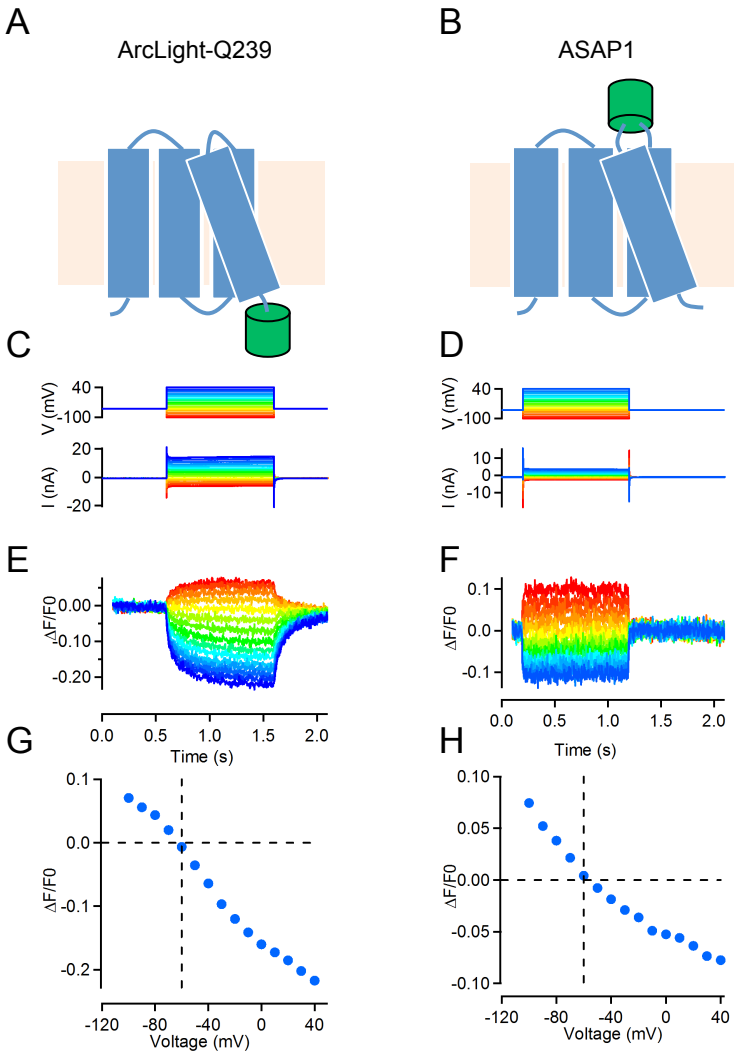

Figure 4. CiVSP-based scaffolds used in the first phase of screening. (A) Topology of ArcLight-Q239 protein at membrane with intracellular FP. (B) Topology of ASAP1 protein at membrane with extracellular FP. (C) Voltage clamp experiment of HEK293T cell expressing ArcLight-Q239. Voltage steps (to -100 to 40 mV from -60 mV holding potential; top) and membrane currents (bottom). (D) Same as (C) for ASAP1. (E) ArcLight-Q239 fluorescence responses to voltage steps (fluorescence traces, top; $\Delta F/F_0$ traces after correction for bleaching, bottom).(F) Same as (E) for ASAP1. (G) ArcLight-Q239 fluorescence changes versus voltage steps from -60 mV holding potential.(H) Same as (G) for ASAP1.

(CAG), sensor cDNA, and a fluorescent protein localized to the nucleus to control for expression levels (**Fig. 5B**). The crystal structures of *C. intestinalis* voltage sensitive phosphatase guide the site-directed mutagenesis. The gating charge positions that mediate torsional movement of helix S4 are known, and they and nearby residues will be mutated first in our priority list. Mutating the R0 (R217E) charge, for example, is known to negatively shift the $V_{1/2}$ by 120 mV. Engineering these residues will affect the range of voltage of sensing.

Our methods and budget allows for ~10^5 variants per year (with 8 replicated wells per variant). Given our throughput we will be able to explore many alterations including: point mutants, randomization of linker and other domains, domain swaps from different voltage-sensitive proteins, combinatorial point mutants, etc. To completely explore the residue space at each position singly of a 500 amino acid sensor protein requires 9,500 constructs. Thus our throughput

is well-matched to our goals. Mutant libraries are constructed with some redundancy among clones, which serve as internal controls in screening. That is, a residue substitution occurs 3.5 times on average in a library. All mutant constructs will be fully sequenced by deep sequencing at a cost of ~$0.08 per construct. After sequencing, redundant constructs will be excluded to increase imaging throughput. Mutants that improve performance in any of the screened parameters will be combined. Prior experience has shown that mutations can be additive. Should performance of an intermediate mutant reach sufficiently high levels over the starting materials, it may become the new scaffold molecule (before completion of saturation mutagenesis); the flexibility of our pipeline allows us to respond quickly to such developments.

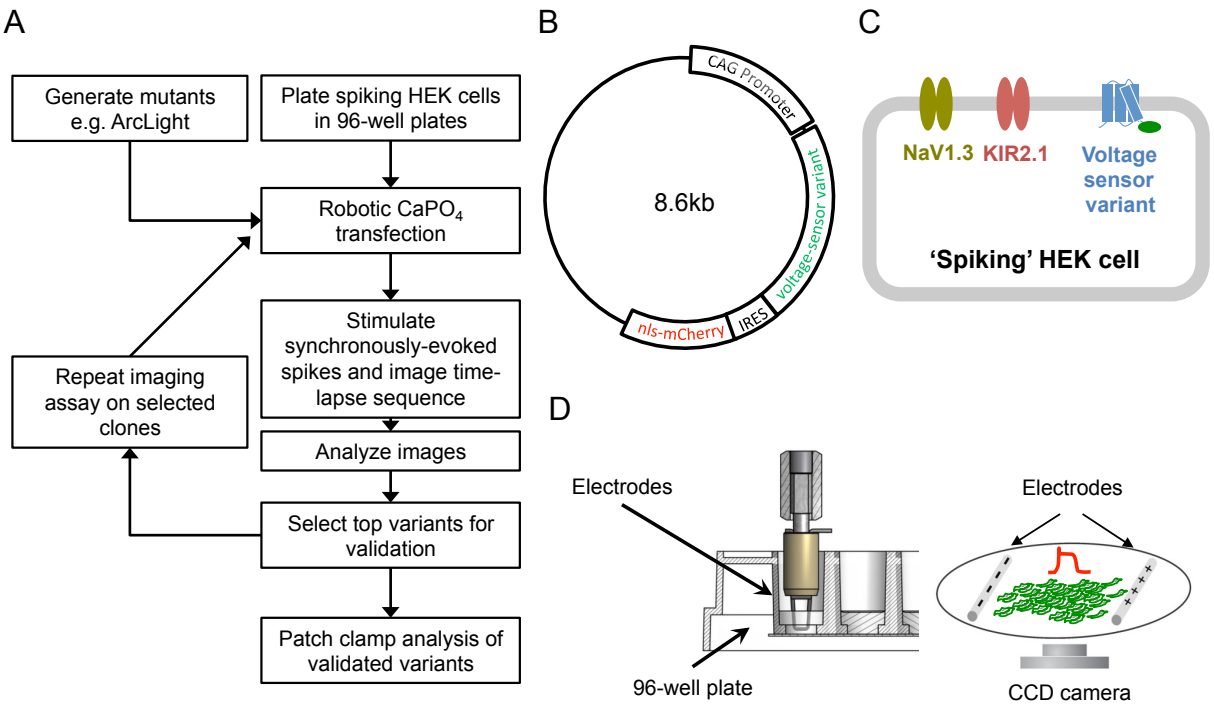

Figure 5. High-throughput screening for improved GEVIs.
(A) Flow chart. (B) Expression vector with CAG promoter, voltage-sensor variant, internal ribosome entry site (IRES), nuclear localization signal (nls) fused with mCherry. (C) 'Spiking' human embryonic kidney (HEK293T) cell stably expressing voltage-gated sodium channels (NaV1.3) and inward-rectifier potassium channels (KIR2.1). One voltage sensor variant is transiently transfected into cells in each well. (D) Schematic of stimulation geometry with an electrode in one well of a 96-well plate. ArcLight variant cells (green). Evoked action potential (red).

Screening for improved voltage sensor function

Voltage sensor screening is based on tissue culture cells (**Fig. 5C**). Tissue culture cells were chosen for their ready supply and ease of gene transfection, enabling high-throughput testing. To produce standardized membrane potential changes we use human embryonic kidney (HEK293T) cells that have been rendered spiking through stable transfection of a voltage-gated sodium channel and inward rectifying potassium channel (**Fig. 5C**) (56). Field stimuli evoked from an inserted electrode reliably trigger action potentials (-80 to 60 mV) with fast rise times ($t_{1/2}$ < 1 ms)(**Fig. 5D; Fig. 6**), which cause a plateau potential, followed by a relatively slow return to baseline with a few seconds. Our assay takes advantage of the consistency of spike onset and amplitude in these cells.

Imaging and field stimulation is performed in 96 well plates in a fully automated manner (**Fig. 7**). We image the responses of several hundred cells per well using a fluorescence microscope and high-speed camera (~100 frames per second, 400 x 400 µm, 128 x 128 pixels, 1 image per well) (**Fig. 8**). Wells are sampled in a serial manner. Imaging time per 96-well plate is 15 minutes. Images from each well are analyzed for changes in fluorescence in response to field stimulation (**Fig. 9**). The most promising sensors (putative hits) are imaged again in independent experiments (**Fig. 5A**).

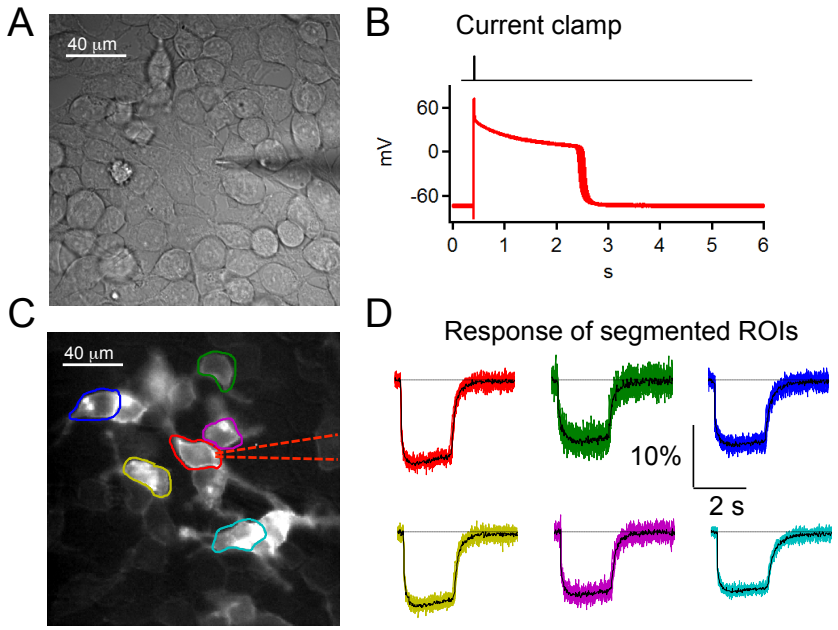

Figure 6. Validation of the electrical stimulation protocol.
(A) Spiking HEK cells and recording pipette. (B) Voltage responses of one cell over multiple trials with field stimulation (1 ms duration, 15 s interstimulus interval). (C) Fluorescence image of cells expressing ArcLight-Q239 in (A). Pipette and recorded cell (red). (D) Fluorescence traces of outlined cells in (C).

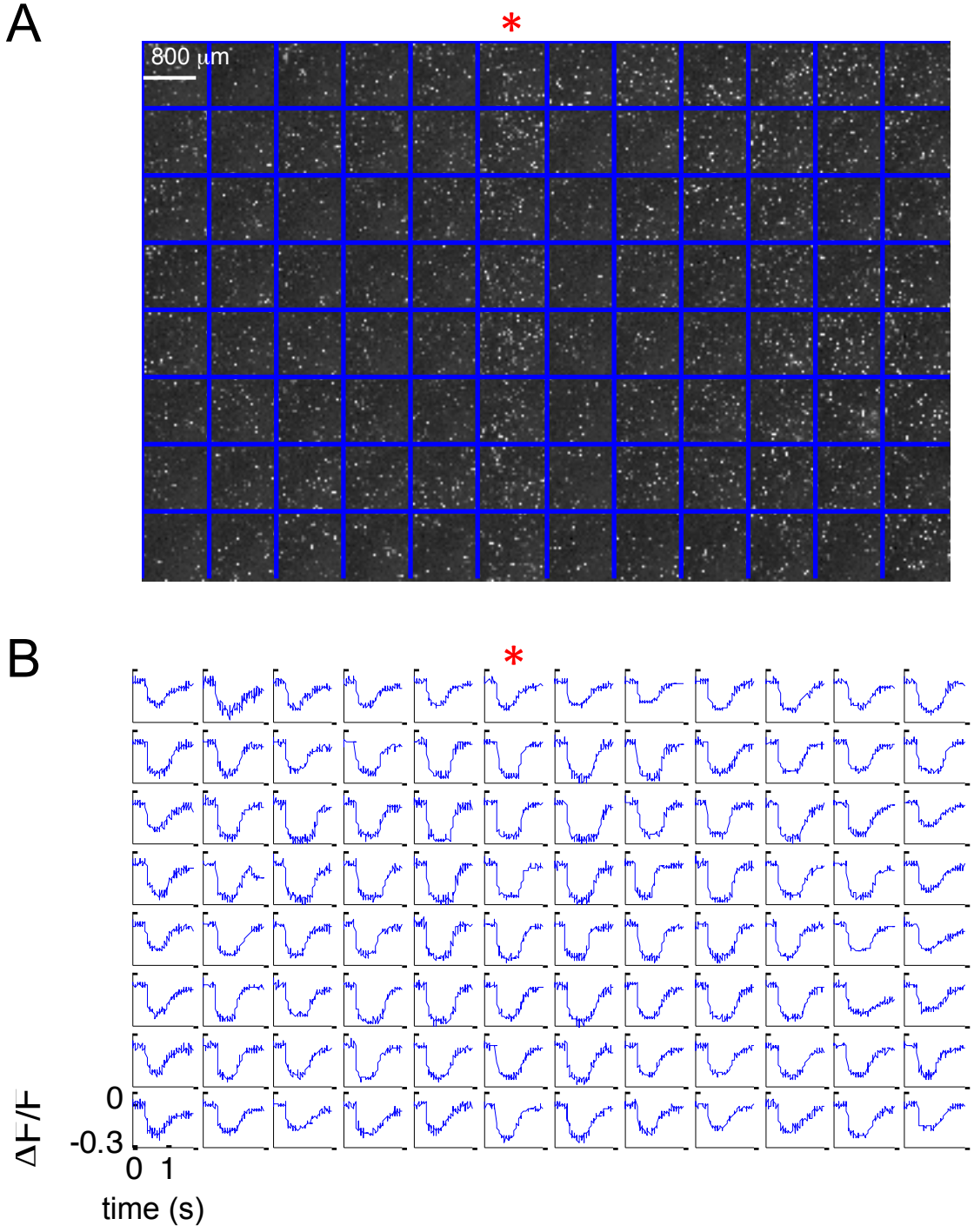

Figure 7. Format of the screening data
(A) Fluorescence image of 96-well plate with spiking HEK cells expressing a different ArcLight variant in each column. The control ArcLight construct is present in column 6 (red asterisk). An individual field-of-view from a well is shown in each square (blue). (B) Fluorescence traces from 96-well plate. Average $\Delta F/F_0$ response of all cells is shown for each well.

We have tuned the assay so that we can now detect 10% improvements in sensitivity with six replicates (**Fig. 10A**). Our assay readily picks up known differences between different sensor variants (**Fig. 10B**). The sensitivity of the screen is stable over extended periods of time (**Fig. 10C**). The demonstrated throughput is 384 variants tested per week (8 replicate wells per variant), limited by the cloning rate. We expect throughput to increase to 2,000 variants tested per week.

We have screened > 4,000 variants of ArcLight-Q239 (**Fig. 11**). The screen has identified multipleArcLight-Q239 variants with improved response amplitude, signal-to-noise ratio, or with faster kinetics. These variants have been confirmed in independent runs. The most promising hits are being validated by patch pipette recordings of transfected HEK cells (**Fig. 4**). Overall, 40 of 480 amino acid positions have been interrogated in the 4,000 point mutants assayed, including positions on all helices of the VSD and extracellular loops.

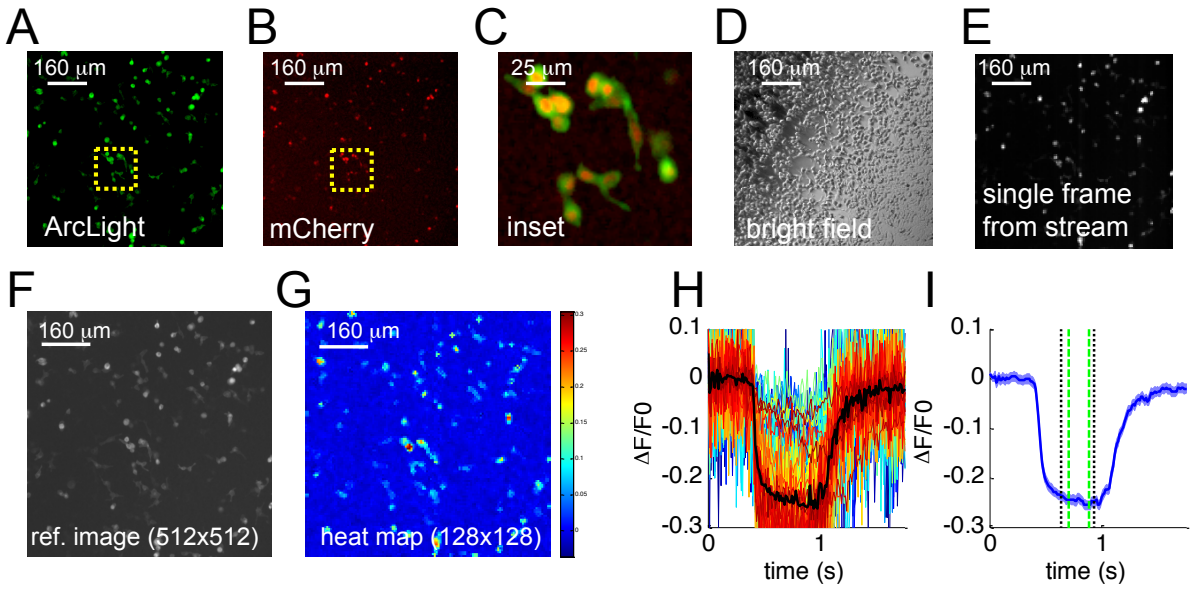

Figure 8. Screening data from a single well.
(A) ArcLight fluorescence in transfected spiking HEK cells. (B) Nuclear mCherry fluorescence. (C) Merged image of ArcLight and nls-mCherry. Zoomed-in image from insets in (A) and (B). (D) Bright field image of same field showing cell density. (E) Single frame of image stream. ArcLight fluorescence at low resolution (4x4 binned). (F) Same as (A). (G) Peak $\Delta F/F_0$ map of same field (4x4 binned). (H) ΔF/F0 traces from ROIs. Average trace (black). (I) Average response (blue) and s.e.m. (light blue).

Screening challenges

Due to the relatively poor membrane targeting of VSD-based constructs (which are obligate dimers, among other potential pitfalls), higher GEVI expression leads to higher fractions of non-productive intracellular fluorescence and thus smaller signal levels. Variability in expression therefore causes variability in the screening results. Achieving tighter control over sensor expression in spiking HEK cells will reduce this variability. Lentiviral or mammalian-compatible baculoviral (BacMam) vectors could improve uniformity of gene transduction and sensor copy number per cell.

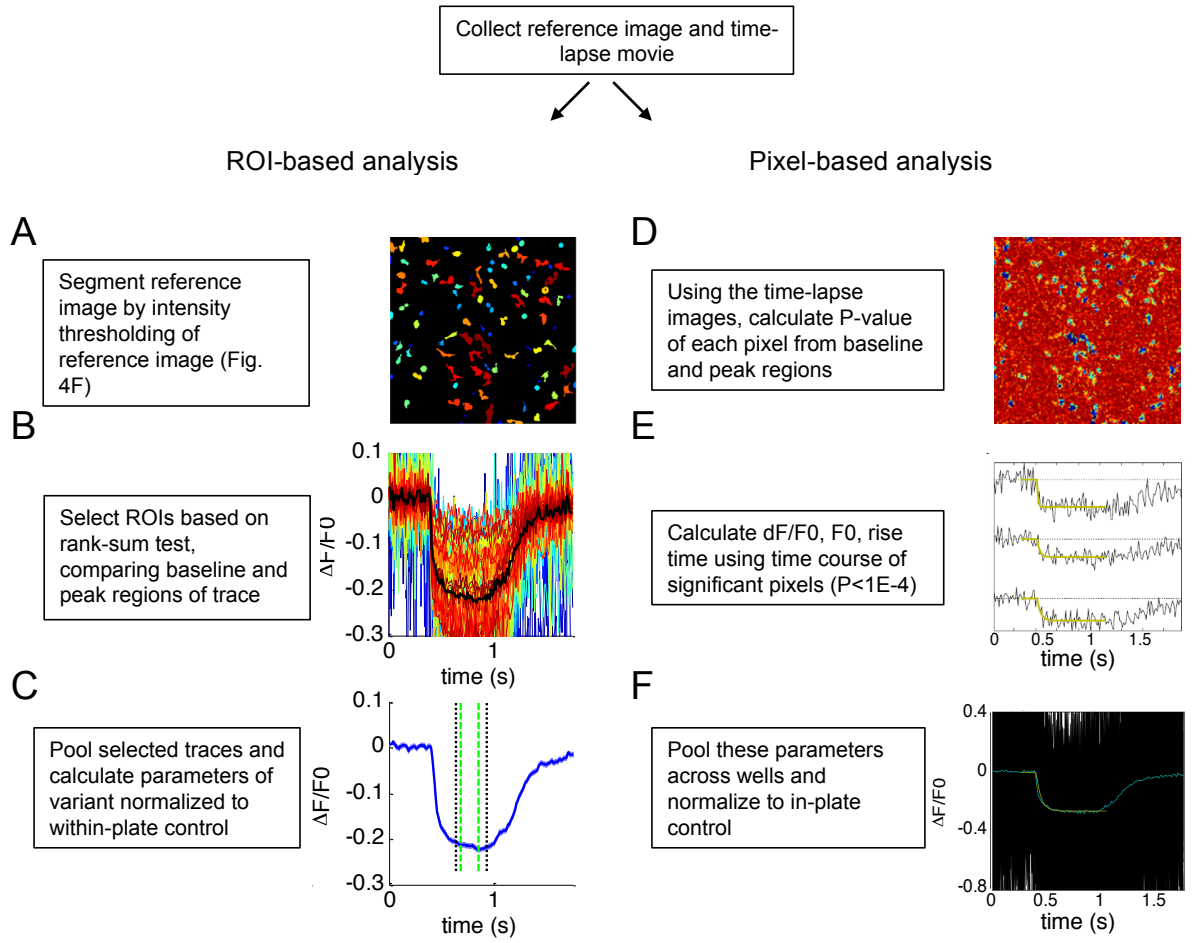

Figure 9. Analysis pipelines.
Two separate analyses are performed because they pick up a separate set of hits. (A) For intensity-based analysis, ROIs are segmented based on thresholding of F_0. Each ROI is colored differently. (B) $\Delta F/F_0$ traces of ROIs. Average trace (black). ROIs are then selected based on rank-sum test comparing F_{peak} to F_0. This is to remove dead cells an fluorescent junk from the analysis. (C) Filtered traces. Average (blue) and s.e.m. (light blue). Frames averaged to define peak (between gray or green lines). (D) For the separate pixel-based analysis, individual pixels are filtered based on rank-sum test. P-value for each pixel is represented by color in map. (E) Example $\Delta F/F_0$ traces of some filtered pixels. Single exponential fit of each trace (yellow). (F) All traces from all filtered pixels and wells (black). Average trace (cyan). F_0, $\Delta F/F_0$, and rise time are averaged across all filtered pixels.

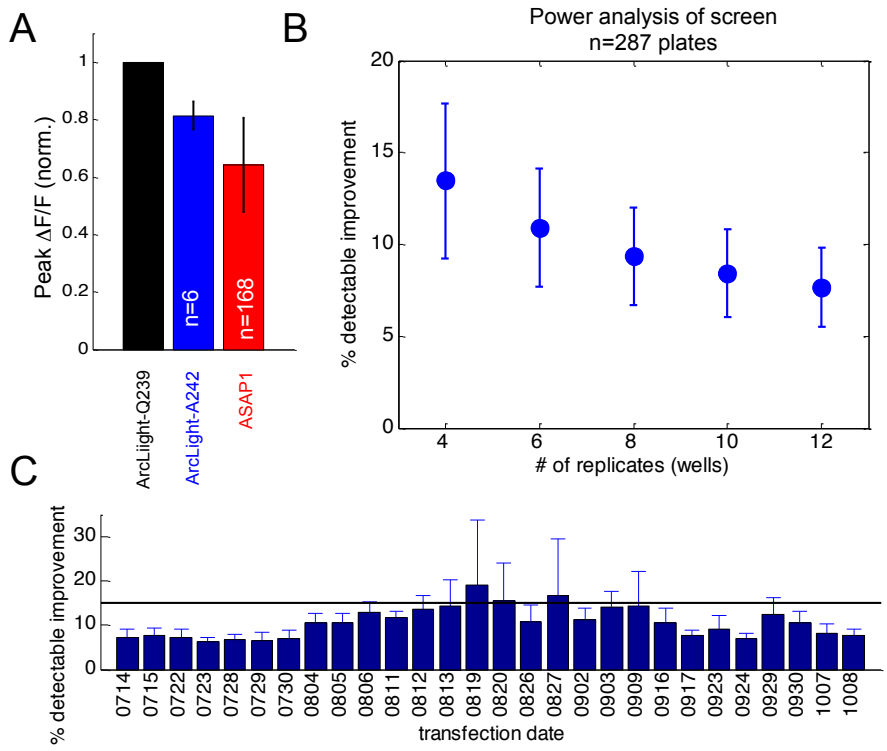

Figure 10. Screen sensitivity and consistency.
(A) Average responses across wells of previously characterized GEVIs. ArcLight-Q239 (black), ArcLIght-A242 (blue), ASAP1 (red). Intensity-based segmentation was used.
(B) Detection sensitivity. The plot shows the detectable improvement compared to ArcLight-Q239 as a function of the number of replicate wells. Percent detectable improvement was estimated by computing 10^5 averages using 4 to 12 replicate wells from a data set of 8 wells per plate. The difference between the mean and the 99th percentile of the distribution of averages normalized by the mean defined the detection sensitivity at α=0.01 for a plate. Data shown are the detection sensitivities averaged across 287 plates.
(C) Detection sensitivity over time. Each transfection date corresponds to 4-32 imaged plates.

The primary screening parameter is the fluorescence change per action potential, $\Delta F/F_0$. In our screen this factor is polluted by membrane targeting, which in turn is modulated by trafficking, translation, transcription, and protein degradation. The majority of our $\Delta F/F_0$ hits correlate with lower F_0. Although a mechanistic analysis is still ongoing, this is consistent with lower expression and as a result relatively better membrane targeting; it is also possible that we lowered the per-molecule resting brightness, as was the case in GCaMP5. It may be necessary to improve the screen by measuring additional variables, such as surface expression.

Other parameters to consider include the capacitative loading of cell membranes and other mechanisms of cytotoxicity or perturbation of native neurophysiology. GEVIs containing a VSD or other "voltage paddle" motif will inherently increase membrane capacitance. For example, ArcLight-expressing cells are slower to return to resting potential from depolarization than control cells. As with any exogenously expressed sensor, GEVIs will alter (at least somewhat) the very thing that they seek to measure. We will keep an eye on the effect of GEVI candidate expression on cell parameters, including resting membrane potential, capacitance and morphology.

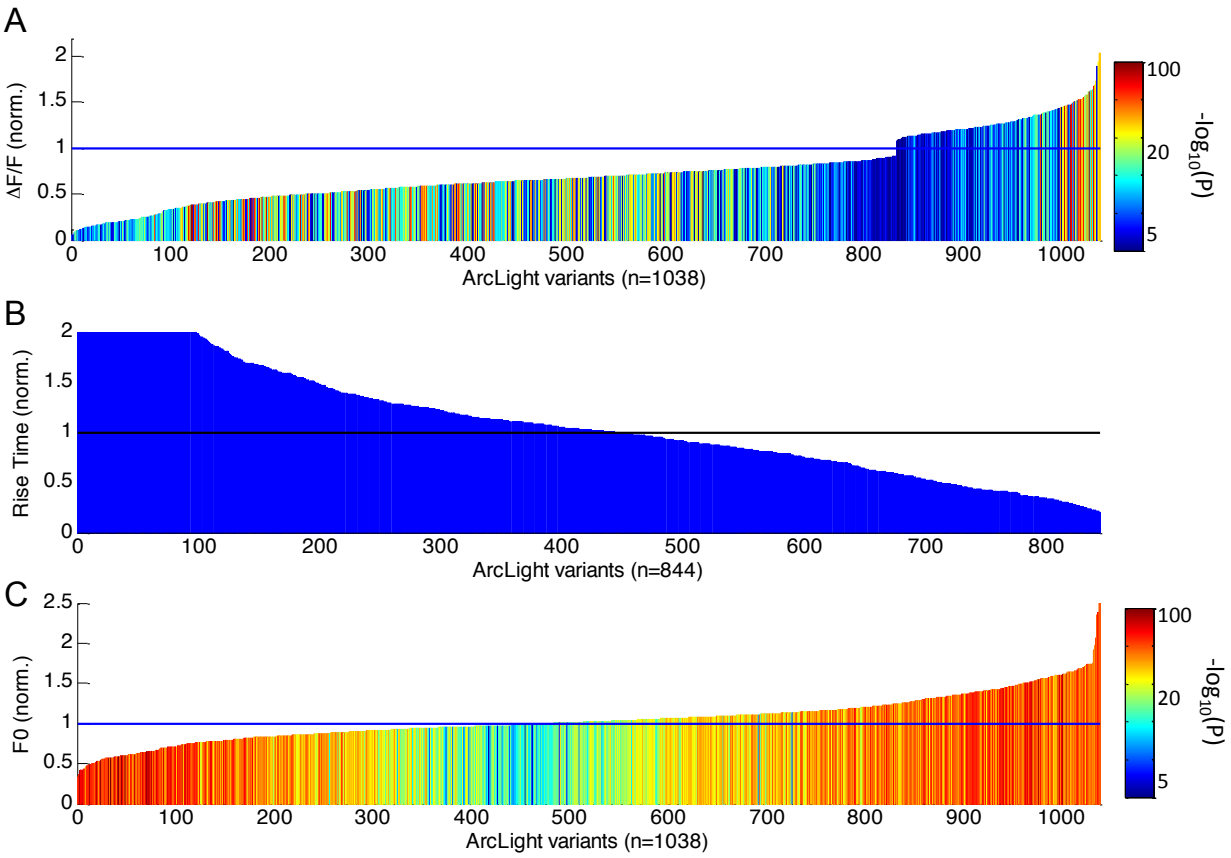

Figure 11. Screening results.
(A) Peak $\Delta F/F_0$ for 1038 ArcLight variants (normalized to control ArcLight response) that exhibit significantly different peak amplitudes compared to wild-type ArcLight (ranksum test, P<1E-5).
(B) Rise time for 844 variants.
(C) F_0 for the 1038 variants shown in panel A.

Additional prototype voltage sensors

It is possible that suitable GEVI scaffolds may not currently exist. We will develop additional scaffolds, including direct placement of FP chromophores into the membrane. One approach might include targeted modification of the FP surface to increase lipophilicity and membrane intercalation. Potential designs include "stapling" FPs between transmembrane helices alongside specific intra-cellular and extra-cellular targeting domains; inserting FPs into the middle of pore-forming proteins, such as has been done inside designed cavitated chaperonins (53); or by reengineering FP surface residues to be more hydrophobic and/or be targeted for fatty acid attachment (the reverse of this approach has been used successfully to reengineer G-protein coupled receptors (obligate membrane proteins) to become soluble proteins for high-throughput

drug screening and crystallization (14). FPs that are directly inserted into the membrane bilayer (assuming they retain fluorescence) should *de facto* be optical indicators of membrane potential, as transmembrane voltage will alter the pi-electron density of the FP chromophore, affecting quantum yield, as is the case with small molecule voltage dyes acting by charge separation in the membrane. Furthermore, voltage-dependent rearrangement of side-chains might alter the pK_a of the chromophore, contributing extinction coefficient changes as well.

Other potential voltage-dependent proteins could be used as scaffolds instead of VSDs. One candidate is prestin, the protein that drives electromotility of the outer hair cells in the ear. Prestin functions by undergoing a profound conformational change upon depolarization, going from an extended conformation to a contracted one, with individual protein monomers predicted to move by 30-70 Angstroms (compared to the ~1-2 Angstrom movement of the VSD) (57). Prestin thus offers the possibility of much larger effects on FP conformation and thus fluorescence. Prestin has been successfully tagged with GFP, while retaining membrane targeting and function, which suggests that a path to a fluorescent sensor is possible. Our tissue culture-based screen is ideal to help discover new voltage sensor variants.

Even restricting ourselves to VSD-based sensors, there are opportunities for substantial improvement through alteration of sensor topology. FPs can be inserted into loops (as was done with ASAP1), additional membrane-tethering motifs can increase allosteric modulation through conformational restriction, and repacking of the VSD/FP interface could improve signal change, brightness and/or stability, as has been the case with GCaMP, RCaMP and RGECO.

Our goal is to develop a set of voltage sensors that reliably detect a single AP and have a range of decay kinetics (1, 10, 100 milliseconds) suitable for a variety of experimental situations. The goals of the project will be met when we have indicators that can measure AP trains in populations of neurons in the intact mouse and *Drosophila* brain, and that can be used to measure subthreshold electrical activity in dendritic arbors of individual neurons.

Milestones

For FY2016, we will produce a standardized benchmarking and screening assay, and the performance of current voltage indicators (Arch, ArcLight, ASAP, VSFP) will be compared. For

FY2017, optimized voltage indicator variants will be made that can detect subthreshold activity of hundreds of neurons *in vivo*. Improved voltage sensor variants will be engineered for high fidelity tracking of neuronal spikes at 100 Hz *in vivo*. For FY2018, 10 best variants will be tested in fly and mouse *in vivo.*

4.3 Publication and Reagent Distribution Plan

Our goal is to produce well-characterized and quality-controlled reagents and make them immediately and widely available to the research community. For example, GCaMP5 was available at Addgene.org for almost one year before publication of the relevant manuscript (8).

4.3.1 Timeline of Reagent Distribution

0-9 Months After Discovery of a New Sensor

Characterization *in vitro* and *in vivo* requires at least 9 months (including creation of viral vectors, transgenic flies, and worms) after the initial discovery. During this time period, reagents will be made available to key collaborators who are testing and calibrating the sensor using previously agreed upon procedures and standards; one obvious example would be collaborators who test in species/systems not represented on the project team. Additionally, laboratories at JRC will receive access to the reagents for use at JRC. Collaborators including JRC laboratories will not distribute the reagents and will not publish results using the sensors prior to publication of the sensors by the project. Our goal is to complete testing within 9 months of initial characterization in cultured neurons.

Transgenic mouse production will be initiated during this period, but production and testing will take considerably longer. Reagents will be distributed to other rodent labs if they plan to create transgenic mice that are not the same as those created at JRC by the project, mainly to avoid duplication of effort, and are willing to widely share these mice on a pre-publication basis (*i.e.* via deposition at The Jackson Laboratory).

9 Months After Discovery

- DNA reagents will be deposited in Addgene, Inc.
- Viruses will be deposited in the University of Pennsylvania Viral Vector Core.
- Flies will be submitted to the Bloomington *Drosophila* Stock Center and/or JRC's shared *Drosophila* resource after validation.

Transgenic mice will be deposited at The Jackson Laboratory as soon as they have been characterized, no later than 9 months after germline transmission.

Reagents that have been tested, but are not being pursued further, will be advertised on the JRC website and made available through Addgene, Inc., or the University of Pennsylvania Viral Vector Core.

4.7.2 Publication Policies

The generation and characterization of new reagents will be published as a collaboration among the relevant GENIE members and other contributors at JRC and elsewhere. The GENIE Project at JRC will be listed as the first address, unless an alternative is mutually agreed upon. If the manuscript is accepted less than 9 months after discovery, all materials will be distributed without restrictions as described above.

5.0 References

1. Nakai J, Ohkura M, & Imoto K (2001) A high signal-to-noise Ca(2+) probe composed of a single green fluorescent protein. *Nat Biotechnol* 19(2):137-141.
2. Pologruto TA, Yasuda R, & Svoboda K (2004) Monitoring neural activity and [Ca2+] with genetically encoded Ca2+ indicators. *J Neurosci* 24(43):9572-9579.
3. Ohkura M, Matsuzaki M, Kasai H, Imoto K, & Nakai J (2005) Genetically encoded bright Ca2+ probe applicable for dynamic Ca2+ imaging of dendritic spines. *Anal Chem* 77(18):5861-5869.
4. Reiff DF, *et al*. (2005) In vivo performance of genetically encoded indicators of neural activity in flies. *J Neurosci* 25(19):4766-4778.
5. Tallini YN, *et al*. (2006) Imaging cellular signals in the heart in vivo: Cardiac expression of the high-signal Ca2+ indicator GCaMP2. *Proc Natl Acad Sci U S A* 103(12):4753-4758.
6. Mao T, O'Connor DH, Scheuss V, Nakai J, & Svoboda K (2008) Characterization and subcellular targeting of GCaMP-type genetically-encoded calcium indicators. *PLoS ONE* 3(3):e1796.
7. Tian L, *et al*. (2009) Imaging neural activity in worms, flies and mice with improved GCaMP calcium indicators. *Nat Methods* 6(12):875-881.
8. Akerboom J, *et al*. (2012) Optimization of a GCaMP Calcium Indicator for Neural Activity Imaging. *The Journal of neuroscience : the official journal of the Society for Neuroscience* 32(40):13819-13840.
9. Chen TW, *et al*. (2013) Ultrasensitive fluorescent proteins for imaging neuronal activity. *Nature* 499(7458):295-300.
10. Akerboom J, *et al*. (2009) Crystal structures of the GCaMP calcium sensor reveal the mechanism of fluorescence signal change and aid rational design. *J Biol Chem* 284(10):6455-6464.
11. Wang Q, Shui B, Kotlikoff MI, & Sondermann H (2008) Structural basis for calcium sensing by GCaMP2. *Structure* 16(12):1817-1827.
12. Stosiek C, Garaschuk O, Holthoff K, & Konnerth A (2003) In vivo two-photon calcium imaging of neuronal networks. *Proc Natl Acad Sci U S A* 100(12):7319-7324.
13. Seelig JD & Jayaraman V (2013) Feature detection and orientation tuning in the Drosophila central complex. *Nature*.
14. Svoboda K, Denk W, Kleinfeld D, & Tank DW (1997) In vivo dendritic calcium dynamics in neocortical pyramidal neurons. *Nature* 385:161-165.
15. Petreanu L, *et al*. (2012) Activity in motor-sensory projections reveals distributed coding in somatosensation. *Nature* 489(7415):299-303.
16. Cox CL, Denk W, Tank DW, & Svoboda K (2000) Action potentials reliably invade axonal arbors of rat neocortical neurons. *Proc Natl Acad Sci U S A* 97(17):9724-9728.
17. Seelig JD, *et al*. (2010) Two-photon calcium imaging from head-fixed Drosophila during optomotor walking behavior. *Nat Methods* 7(7):535-540.
18. Haag J & Borst A (2000) Spatial distribution and characteristics of voltage-gated calcium signals within visual interneurons. *J Neurophysiol* 83(2):1039-1051.
19. Yuste R & Denk W (1995) Dendritic Spines as Basic Functional Units of Neuronal Integration. *Nature* 375(6533):682-684.

20. Jia H, Rochefort NL, Chen X, & Konnerth A (2010) Dendritic organization of sensory input to cortical neurons in vivo. *Nature* 464(7293):1307-1312.
21. Akerboom J, *et al*. (2013) Genetically encoded calcium indicators for multi-color neural activity imaging and combination with optogenetics. *Front Mol Neurosci* 6:2.
22. Zhao Y, *et al*. (2011) An expanded palette of genetically encoded Ca(2) indicators. *Science* 333(6051):1888-1891.
23. Li H, Li Y, Lei Z, Wang K, & Guo A (2013) Transformation of odor selectivity from projection neurons to single mushroom body neurons mapped with dual-color calcium imaging. *Proc Natl Acad Sci U S A* 110(29):12084-12089.
24. Huber D, *et al*. (2012) Multiple dynamic representations in the motor cortex during sensorimotor learning. *Nature* 484(7395):473-478.
25. Zariwala HA, *et al*. (2012) A Cre-Dependent GCaMP3 Reporter Mouse for Neuronal Imaging In Vivo. *The Journal of neuroscience : the official journal of the Society for Neuroscience* 32(9):3131-3141.
26. Dana H, *et al*. (2014) Thy1-GCaMP6 Transgenic Mice for Neuronal Population Imaging In Vivo. *PloS ONE* 9(9):e108697.
27. Madisen L, *et al*. (2015) Transgenic mice for intersectional targeting of neural sensors and effectors with high specificity and performance. *Neuron* 85(5):942-958.
28. Wu JY, Cohen LB, & Falk CX (1994) Neuronal activity during different behaviors in Aplysia: a distributed organization? *Science* 263(5148):820-823.
29. Popovic MA, Carnevale N, Rozsa B, & Zecevic D (2015) Electrical behaviour of dendritic spines as revealed by voltage imaging. *Nat Commun* 6:8436.
30. Siegel MS & Isacoff EY (1997) A genetically encoded optical probe of membrane voltage. *Neuron* 19:735-741.
31. Dimitrov D, *et al*. (2007) Engineering and characterization of an enhanced fluorescent protein voltage sensor. *PLoS ONE* 2:e440.
32. Tsutsui H, Karasawa S, Okamura Y, & Miyawaki A (2008) Improving membrane voltage measurements using FRET with new fluorescent proteins. *Nat Methods* 5(8):683-685.
33. Jin L, *et al*. (2012) Single action potentials and subthreshold electrical events imaged in neurons with a fluorescent protein voltage probe. *Neuron* 75(5):779-785.
34. Knopfel T (2012) Genetically encoded optical indicators for the analysis of neuronal circuits. *Nature reviews. Neuroscience* 13(10):687-700.
35. St-Pierre F, *et al*. (2014) High-fidelity optical reporting of neuronal electrical activity with an ultrafast fluorescent voltage sensor. *Nat Neurosci* 17(6):884-889.
36. Kralj JM, Douglass AD, Hochbaum DR, Maclaurin D, & Cohen AE (2012) Optical recording of action potentials in mammalian neurons using a microbial rhodopsin. *Nature methods* 9(1):90-95.
37. Gong Y, Wagner MJ, Zhong Li J, & Schnitzer MJ (2014) Imaging neural spiking in brain tissue using FRET-opsin protein voltage sensors. *Nat Commun* 5:3674.
38. Zou P, *et al*. (2014) Bright and fast multicoloured voltage reporters via electrochromic FRET. *Nat Commun* 5:4625.
39. Wardill TJ, *et al*. (2013) A neuron-based screening platform for optimizing genetically-encoded calcium indicators. *PloS one* 8(10):e77728.
40. Gibson DG, *et al*. (2009) Enzymatic assembly of DNA molecules up to several hundred kilobases. *Nature methods* 6(5):343-345.

41. Ding J, Luo AF, Hu L, Wang D, & Shao F (2014) Structural basis of the ultrasensitive calcium indicator GCaMP6. *Science China. Life sciences* 57(3):269-274.
42. Fosque BF, *et al*. (2015) Neural circuits. Labeling of active neural circuits in vivo with designed calcium integrators. *Science* 347(6223):755-760.
43. Thestrup T, *et al*. (2014) Optimized ratiometric calcium sensors for functional in vivo imaging of neurons and T lymphocytes. *Nature methods* 11(2):175-182.
44. Sun XR, *et al*. (2013) Fast GCaMPs for improved tracking of neuronal activity. *Nat Commun* 4:2170.
45. Kredel S, *et al*. (2009) mRuby, a bright monomeric red fluorescent protein for labeling of subcellular structures. *PloS one* 4(2):e4391.
46. Shaner NC, *et al*. (2008) Improving the photostability of bright monomeric orange and red fluorescent proteins. *Nat Methods* 5(6):545-551.
47. Wu J, *et al*. (2013) Improved orange and red Ca(2)+/- indicators and photophysical considerations for optogenetic applications. *ACS chemical neuroscience* 4(6):963-972.
48. Caroni P (1997) Overexpression of growth-associated proteins in the neurons of adult transgenic mice. *J Neurosci Methods* 71(1):3-9.
49. Tsien JZ, *et al*. (1996) Subregion- and cell type-restricted gene knockout in mouse brain [see comments]. *Cell* 87(7):1317-1326.
50. Yasuda R, *et al*. (2004) Imaging calcium concentration dynamics in small neuronal compartments. *Sci STKE* 2004(219):pl5.
51. Sankaranarayanan S, De Angelis D, Rothman JE, & Ryan TA (2000) The use of pHluorins for optical measurements of presynaptic activity. *Biophys J* 79(4):2199-2208.
52. Wilt BA, Fitzgerald JE, & Schnitzer MJ (2013) Photon shot noise limits on optical detection of neuronal spikes and estimation of spike timing. *Biophys J* 104(1):51-62.
53. Peron SP, Freeman J, Iyer V, Guo C, & Svoboda K (2015) A Cellular Resolution Map of Barrel Cortex Activity during Tactile Behavior. *Neuron* 86(3):783-799.
54. Mutze J, *et al*. (2012) Excitation spectra and brightness optimization of two-photon excited probes. *Biophys J* 102(4):934-944.
55. Zeng H, *et al*. (2008) An inducible and reversible mouse genetic rescue system. *PLoS Genet* 4(5):e1000069.
56. Park J, *et al*. (2013) Screening fluorescent voltage indicators with spontaneously spiking HEK cells. *PloS one* 8(12):e85221.
57. Homma K & Dallos P (2011) Evidence that prestin has at least two voltage-dependent steps. *J Biol Chem* 286(3):2297-2307.

6.0 CVs of Project Personnel

CVs for the following people are included in the Appendix:

- Stephan Brenowitz, Senior Scientist (voltage sensor development)
- Hod Dana, Research Specialist (mouse imaging)
- Jeremy Hasseman, Research Specialist (molecular cloning)
- Graham Holt, Research Technician (protein biochemistry)
- Douglas Kim, Program Scientist (project management)
- Yi Sun, Research Specialist (*Drosophila* imaging)
- Getahun Tsegaye, Research Specialist (molecular cloning)